Resonant upscattering effects on ^{238}U absorption rates

Claude Mounier, Pietro Mosca

RESONANT UPSCATTERING EFFECTS ON ^{238}U ABSORPTION RATES

Claude Mounier and Pietro Mosca

Commissariat l'énergie atomique et aux énergies alternatives
CEA Saclay, DEN/DANS/DM2S/SERMA/LLPR, 91191 Gif-sur-Yvette Cedex, France
claude.mounier@cea.fr
pietro.mosca@cea.fr

ABSTRACT

The new requirements of accuracy in reactor physics calculations justify a review of the current models, like that one adopted in the cross-section processing, for a better evaluation of the keff and the resonant absorption rates. In this context, the aim of this paper is to investigate the effects of the free gas kernel developed by Sanchez on the ^{238}U absorption rates. Homogeneous medium tests point out the increase of the absorption rates in the left wing of the resonances due to the upscattering produced by the new kernel. Heterogeneous tests show that the absorption in the left wing of the resonances is mostly affected by the scattering anisotropy in the laboratory system.

Key Words: **Doppler, Free Gas, Resonant Scattering**

1. INTRODUCTION

Modelling the thermal movement of the nucleus in the condensed matter has a long story which starts from Fermi[1] and Wigner-Wilkins [2]. Concerning specifically the free gas (FG) model, it has been later revisited by Finkelstein[3], Blackshaw and Murray[4] theoretically and more recently reanalyzed by Sanchez [5, 6], Dagan[7] and Lee et al[8]. These papers show a numerical approach to consistently calculate the total and the double-differential scattering cross-sections in the framework of the FG model. In this context, the aim of this paper is to investigate the effects of the FG kernel on the ^{238}U absorption rates considering homogeneous medium and heterogeneous tests.

The structure of this paper is as follow. First, some characteristics of the FG kernel are shown through some semi-integral values (upscattering probability and average deviation cosine). Second, some homogeneous medium tests are presented to analyse the spectral changes on the absorption rates of the FG kernel. Then, some heterogeneous tests discuss the effects of the scattering anisotropy order with the FG kernel.

2. FREE GAS MODEL

The starting point is the expression of the total and the double-differential scattering cross-sections supposing that the target is at thermal equilibrium (Maxwellian distribution of speed):

$$\sigma_{s,T}(v) = \frac{1}{v} \int d\vec{V} M_T(\vec{V}) \|\vec{v_r}\| \sigma_{s,T=0}(\|\vec{v_r}\|), \tag{1}$$

$$P_s(\vec{v}, E', \mu_L) = \frac{1}{v\sigma_s(v,T)} \int d\vec{V} M_T(\vec{V}) \|\vec{v_r}\| \sigma_{s,T=0}(\|\vec{v_r}\|) P(\vec{v}, \vec{V}, E', \mu_L), \tag{2}$$

where:

- $M_T(\vec{V})$: Maxwellian distribution of the target velocity $\vec{V}$ at temperature T,

- $\vec{v}$: incident neutron velocity,

- E and E' : neutron energies before and after scattering,

- μ_L : deviation cosine of the neutron in the laboratory system (LAB),

- $\vec{v_r} = \vec{v} - \vec{V}$: relative speed between the neutron and the target.

- $\sigma_{s,T=0}$: scattering cross-section at 0 Kelvin,

- $P(\vec{v}, \vec{V}, E', \mu_L)$: kernel of the two-body elastic scattering,

Nowadays, two models are implemented in the standard NJOY [9] code to calculate expression (2). The former consists in calculating the angular-energy distribution assuming the constancy of the scattering cross-section and the isotropy of the scattering in the center of mass (CM). This approach corresponds to the angular-energy distribution of the classical Wilkins-Wigner model. The latter consists in using a probability transfer calculated under the static assumption (nucleus at rest in the laboratory system) together with the angular distribution of the ENDF-6 evaluation. This model is improperly called static or asymptotic model just to refer to the transfer probability approximation. It is the limit of the FG model when the gas temperature T tends to zero or the ratio of the incident neutron energy over the temperature, E/T, tends to infinity.

A consistent FG model, in which the assumption of a constant nuclear cross-section is removed, has been recently incorporated in NJOY according to the numerical approach proposed by Sanchez in [6]. Equations 1 and 2 are applied up to few hundreds of eV in a similar way as the work of Dagan[7].

The calculation of the probability function Eq. 2, by itself and within the actual framework of NJOY, is very time consuming for two main reasons. Firstly due to the resonant character of the scattering a lot of incident energies must be used to describe properly the energy transfer distribution that is sensitive to the incident neutron energy around the resonance peaks. Secondly,

for each incident neutron energy, a linearisation process of the kernel on the outgoing energy and μ_L is performed prior to the calculation of the multigroup P_N matrices. The first studies, not presented here, have begun with the implementation in the NJOY THERMR module of the pointwise P0 component of the kernel $\sigma_s(E, E')$ that is less time consuming but not rigorous except for infinite medium problems. Considering the incident energy of 6.52 eV, the computing time of the pointwise thermal matrix with the kernel is 16 times higher than with the P0 component. The number of incident energies needed without any prior optimization is equal to 17468 up to 1 keV. These energies correspond to the energy grid of the 0.1% reconstructed scattering cross section at 974 K. Moreover, with the kernel, a reasonable convergence on $\overline{\mu(E)}$ requires a reconstruction accuracy equals to at least 0.05% compared to the usual value of 0.1% and the average computation time of the pointwise thermal matrix at 974 K is around 102 s per incident energy on a workstation (Xeon X5550, 2.67Ghz) in the energy range up to 1 keV.

3. UPSCATTERING PROBABILITY AND AVERAGE DEVIATION COSINE

There are some changes on the angular-energy distribution between the FG and the asymptotic models. This point is discussed analysing these two semi-integral values: the upscattering probability and the average deviation cosine. These values are deduced from the output pointwise file computed by the new NJOY version.

It is reminded that the asymptotic kernel (AK) gives an average deviation cosine $\bar{\mu}$ equal to $\frac{2}{3A}$ and an upscattering probability that is null. The FG model tends to these limits at high energy for a given temperature or at any energy when the temperature tends to zero.

Figure 1 shows the ^{238}U upscattering fraction together with its average deviation cosine in the energy range between 0.1 and 1000 eV at 974 K. One can see that upscattering is present in all the energy range considered and that neutrons are on average slightly backscattered ($\bar{\mu} < 0$) in correspondence to an high upscattering in the two first resonances. If one looks more specifically around some specific resonances, like those ones around 6.67 and 36.68 eV (Fig. 2, 3), one can observe that the upper energy wing of the resonance displays an average forward angular scattering and low upscattering probability while in the lower energy side there is a drastic reduction of the average deviation cosine in correspondence to a high upscattering. The reason for such a result is connected to the kinematics and to the resonant character of the cross-sections. On one side, the highest momentum transfer to a neutron is obtained for a head-on collision (negative deviation cosine), on the other side, these scattering events are weighted by the huge factor $v_r\sigma_{s,T=0}(v_r)$ only if the relative velocities are localized on the left wing of the resonance.
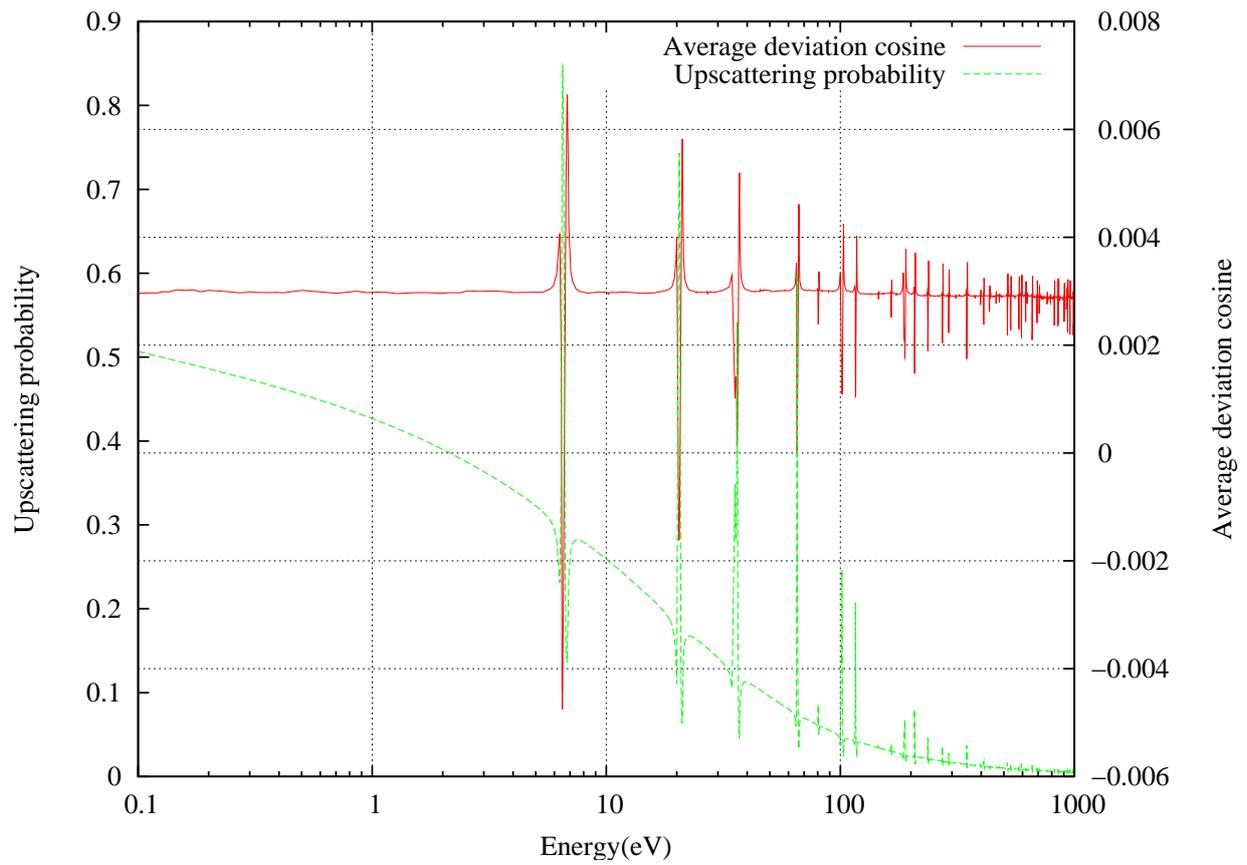
Figure 1. ^{238}U average deviation cosine and upscattering probability at 974 K in the range between 0.1 and 1000 eV
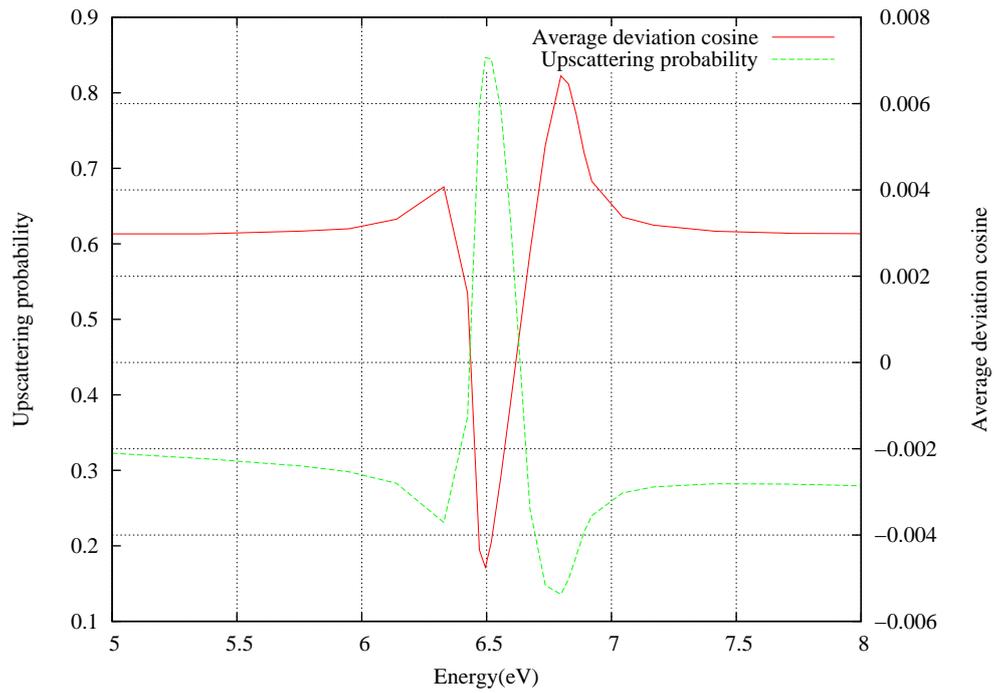
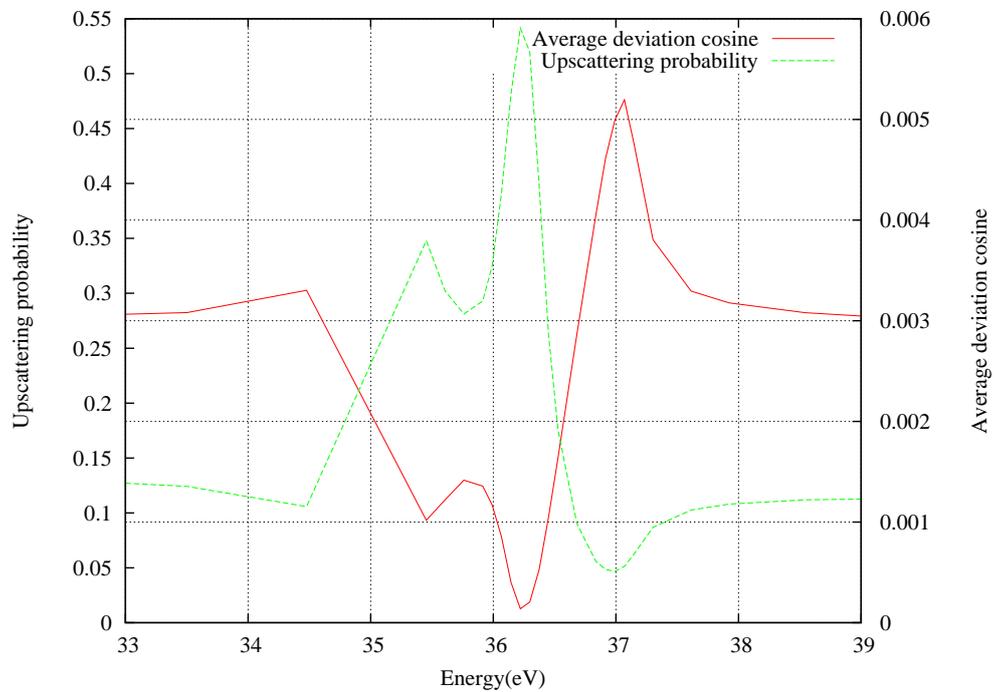**Figure 2.** ^{238}U average deviation cosine and upscattering probability at 974 K in the resonance at 6.67 eV

Figure 3. ^{238}U average cosine of deviation and upscattering probability at 974 K in the resonance at 36.68 eV

4. HOMOGENEOUS TESTS

The homogeneous problems are aimed to show the spectral changes on the absorption rates of the FG kernel. In this perspective, the fine structure equation is used in these tests:

$$(\sigma_t(E) + \sigma_b)\phi(E) = \int \sigma_s(E, E')\phi(E')dE' + \frac{\sigma_b}{E},$$ (3)

where $\sigma_t(E)$ is the total pointwise cross-section, $\sigma_s(E, E')$ is the pointwise matrix transfer and σ_b is the background cross-section. The solution of Eq. (3) is obtained by the pointwise Monte Carlo code TRIPOLI-4®[10] and by the multigroup solver and the subgroup self-shielding module of the AEMC code[11]. Monte Carlo calculations are carried out activating the Doppler Broadening Rejection Correction (DBRC) option [12] and creating a pseudo-nuclide having a constant absorption cross-section of a one barn and a concentration equal to σ_b. The AEMC code uses the multigroup transfer matrix processed by the new NJOY version code. All the multigroup data are produced over the fine UNIVSH11513 [13] energy mesh and for the self-shielding the same pointwise cross-section of TRIPOLI-4®are used as quadratures.

Figures 4 and 5 show that the relative discrepancies of the absorption rates, collapsed over the SHEM281 [14] energy mesh for a background cross-section equal to 50 barns in the range between 4 and 907 eV, are within the three standard deviations of TRIPOLI-4®. These results prove that the DBRC method and the FG kernel are consistent with each other.

Figure 6 shows the relative error on the cumulated ^{238}U absorption at 50 barns versus energy between AK and the FG model. As one can see, in each resonance there is a local oscillation of the relative discrepancy and this oscillation is directly related to the scattering characteristics of the resonance. The highest error is around the resonance at 36 eV which has a high neutron width.

Table I presents the cutoff energies, i.e. the energies from which the error on the cumulated ^{238}U absorption between the AK and FG model are lower than a tolerance ϵ. The cutoff energies, that correspond to the boundaries of the fine energy mesh used in the calculation, increase for higher temperatures and lower background cross-sections. They span between few tens and few hundreds of eV. For standard APOLLO2 multigroup libraries (not used in this study), the thermal cutoff has been fixed at 360 eV, as compromise between the two highest cutoff and the boundaries of the SHEM281 energy mesh, in order to guarantee a correct modelling around the temperatures close to the fuel melting.

Fig. 7 gives some elements of explanation about the oscillations of the discrepancy around the resonances. One can see from the highest graph in Fig. 7 that AK overestimates absorption rates for higher energies of the resonance peak and underestimates for energies below the peak. The first effect is explained by the fact that out of resonances AK gives an average energy loss higher than the FG kernel since upscattering is absent. Thus, a larger number of neutrons is transferred to the right wing of the resonance with AK. The second effect, as illustrated in the graph in the middle of Fig. 7, is a consequence of the energy gain introduced by the FG kernel below the peak of the resonance.
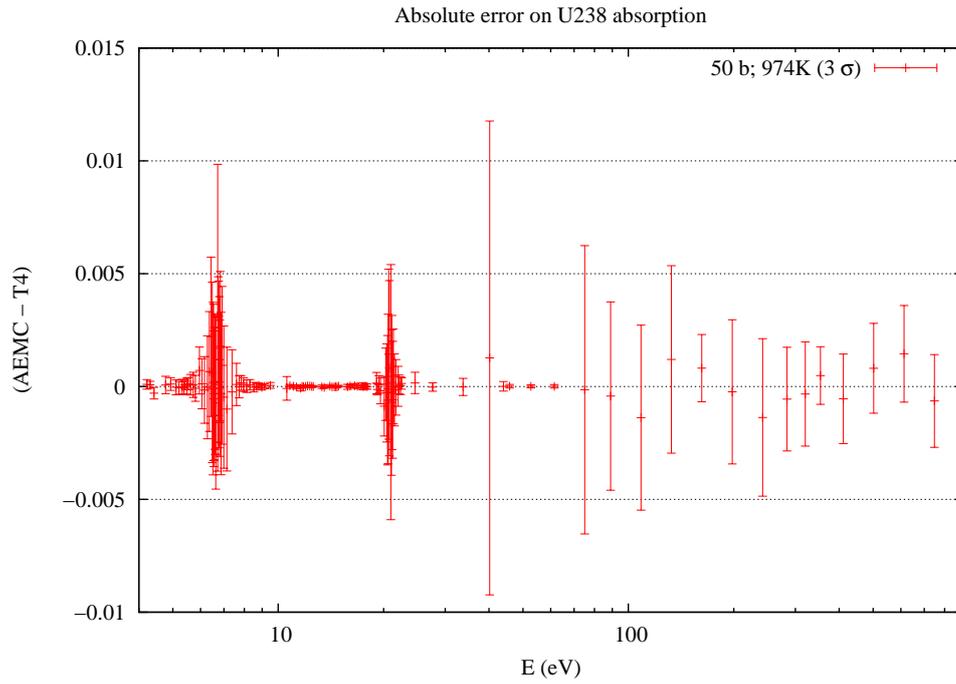
Figure 4. Differential discrepancies between AEMC and TRIPOLI-4 on the ^{238}U absorption between 4 and 907 eV at 974 K and 50 barns
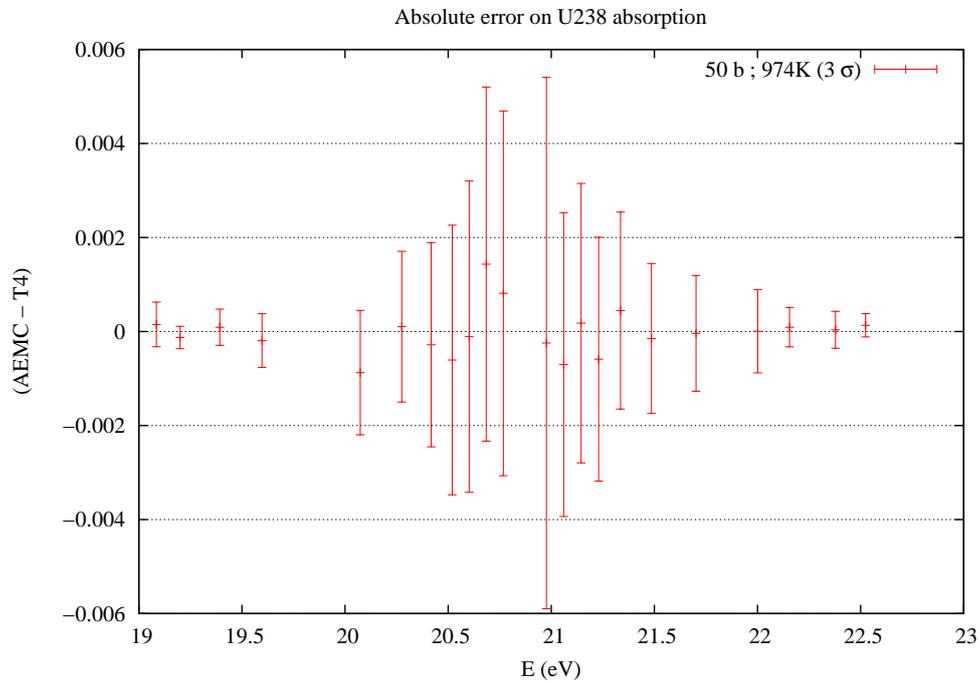

Figure 5. Differential discrepancies between AEMC and TRIPOLI-4 on the ^{238}U absorption in the 20.87 eV resonance at 974 K and 50 barns
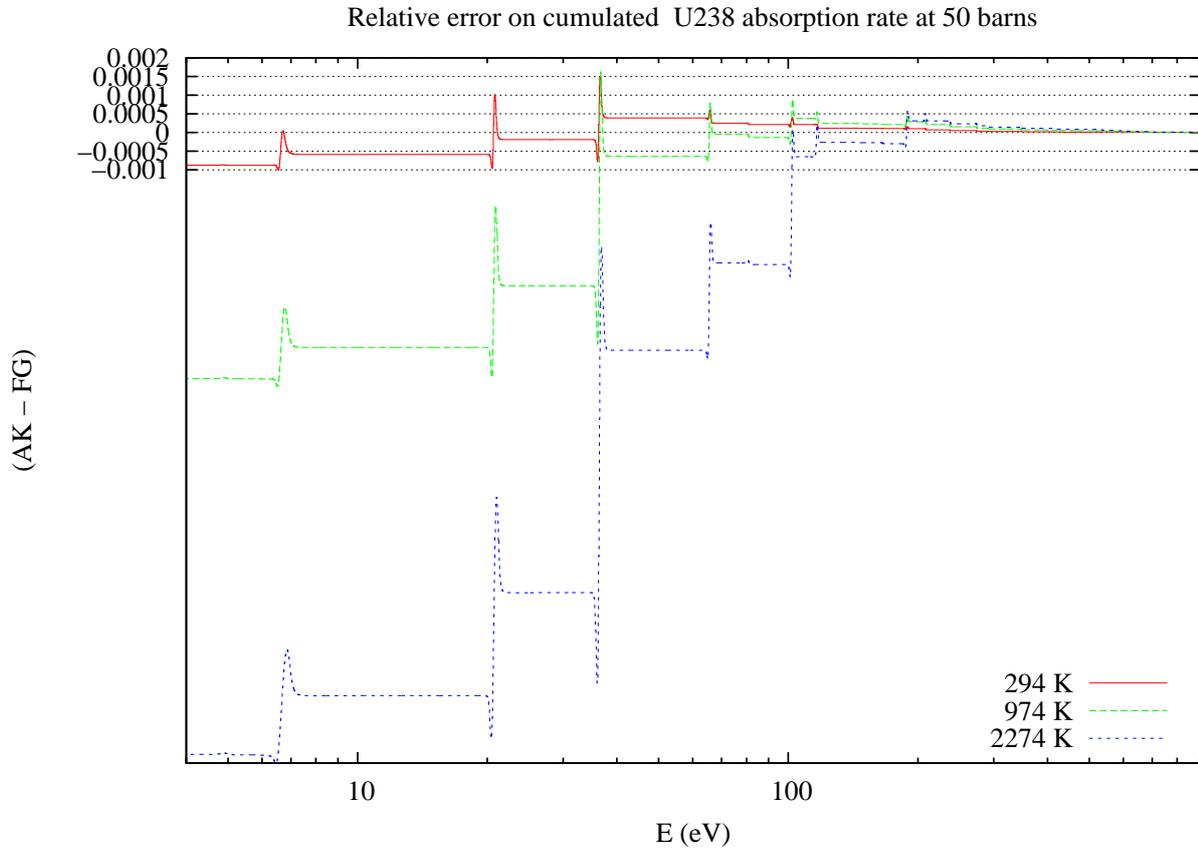
Relative error on cumulated U238 absorption rate at 50 barns

Figure 6. Cumulated error on absorption between asymptotic (AK) and free gas (FG) kernels at 50 barns

Temperature (K)	$E_c(\epsilon[\%])$		
	$E_c(0.1)$ and $\sigma_d = 1$ barn	$E_c(0.05)$ and $\sigma_d = 1$ barn	$E_c(0.05)$ and $\sigma_d = 50$ barns
294	36.803599	66.227491	66.020853
974	117.08350	273.36393	116.83983
2274	290.54007	435.24459	208.18105

Table I. Cutoff energies satisfying the criterium. They correspond strictly to the values of the fine energy mesh used in the calculation.
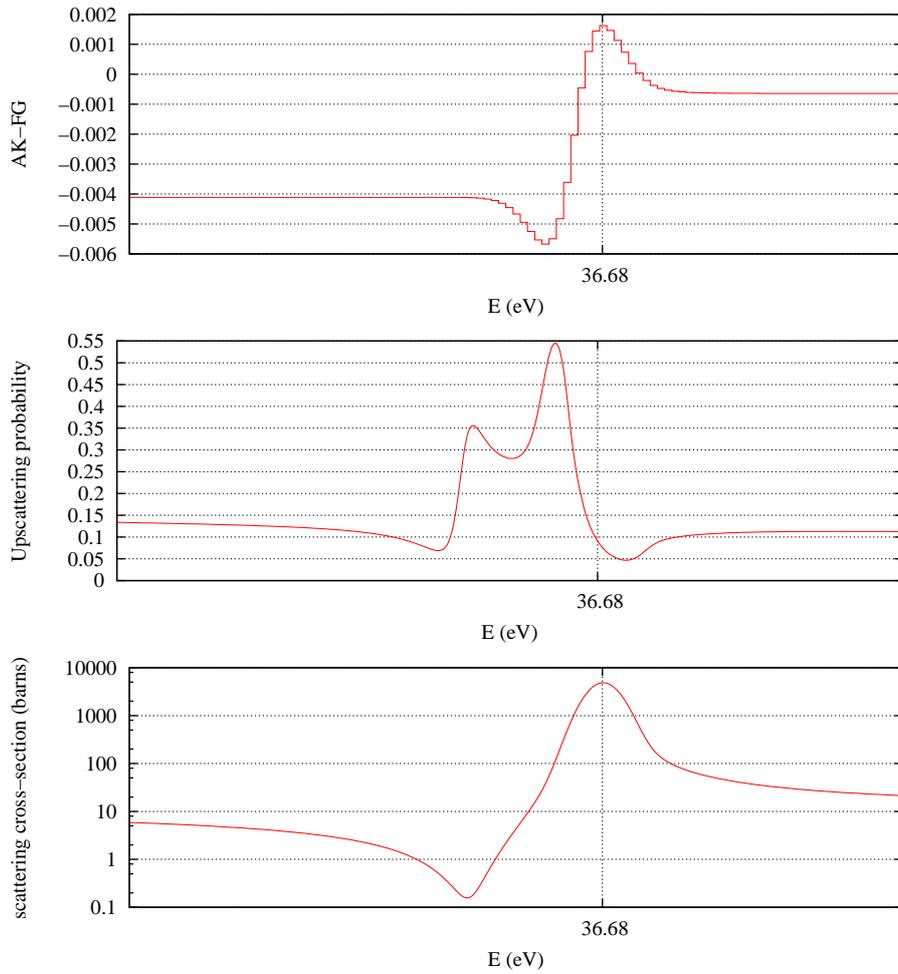
Figure 7. Relative cumulated error on absorption between asymptotic (AK) and free gas (FG) kernels at 50 barns and 974 K around the resonance at 36.68 eV. Below upscattering probability and scattering cross-section

5. HETEROGENEOUS TESTS

A simple square cell model (pitch 1.2619 cm) is considered with a dioxyde fuel rod (0.4096 cm radius), composed of ^{238}U (2.2×10^{-2} at./(barn.cm)) and ^{16}O, and surrounded by light water (1.834×10^{-2} at./(barn.cm)) without cladding. The rod is subdivided into four concentric rings that have fractional volumes equal to 50%, 30%, 15% and 5% from the center to the periphery. The external source between 1 keV and 19.64 MeV is uniform in the moderator and equal to one. The fission source is suppressed by setting ^{238}U neutron multiplicity per fission to zero. ^{238}U was processed according to the FG model up to 1 keV and the standard AK above. The cross-sections of the all the other nuclei were calculated following the standard treatment (AK above 5 eV). Transport calculations were performed by the MOC solver of the APOLLO2 code [15], using a subset of the UNIVSH11513 energy mesh (containing 6211 energy groups) and taking into account an anisotropic scattering order up to P_5.

Since the double-differential cross-sections derived from AK and FG model are significantly different, the aim of these tests is to quantify the differences between these two models in heterogeneous problems, varying some parameters like the temperature and the anisotropic scattering order of ^{238}U.

5.1. Integral Results

Before giving both spectral and spatial details on the ^{238}U absorption rates, some integral results of the rod are presented in Table II. At 294 K, the differences between the two models are low, they become more significant increasing the temperature. At 974 K there is 0.8% more absorption with the FG model compared to AK. The effect of the scattering anisotropy for both models are low at all temperatures.

Model	294 K		974 K		2274 K	
	P_0	P_5	P_0	P_5	P_0	P_5
Free Gas (FG)	18309	18318	20102	20114	22589	22604
Asymptotic Kernel (AK)	18289	18301	19936	19954	22113	22137
(AK - FG)/FG in %	-0.11	-0.09	-0.82	-0.79	-2.11	-2.06

Table II. ^{238}U absorption rates in the rod comparison between FG and AK between 5.5 and 1000 eV in pcm

The absorption in the second ring, which represents around one fourth of the total rod absorption, shows slightly higher differences between the two models at the highest temperatures (Table III) than those of the total absorption.

Model	294 K		974 K		2274 K	
	P_0	P_5	P_0	P_5	P_0	P_5
Free Gas (FG)	5035	5039	5367	5373	6006	6015
Asymptotic Kernel (AK)	5030	5034	5314	5325	5849	5862
(AK - FG)/FG in %	-0.11	-0.09	-0.97	-0.90	-2.63	-2.54

Table III. ^{238}U absorption rates in the second ring comparison between FG and AK between 5.5 and 1000 eV in pcm

5.2. Spectral Results

Figures 8 and 9 illustrate the relative discrepancy in percent on ^{238}U absorption in the four rings and in the rod for the two highest fuel temperatures using a P_5 scattering order. Since the greatest discrepancy is attained around the resonance at 36.68 eV, all the results are analysed in the energy range of this resonance. One can see that the highest discrepancies between the two models are localized in the first and second ring, while the fourth ring is the lowest affected region by the model change. The highest discrepancies are attained in the left side of the resonance and it corresponds to a maximum underestimation of the absorption rates equal to -45 % at 974 K.
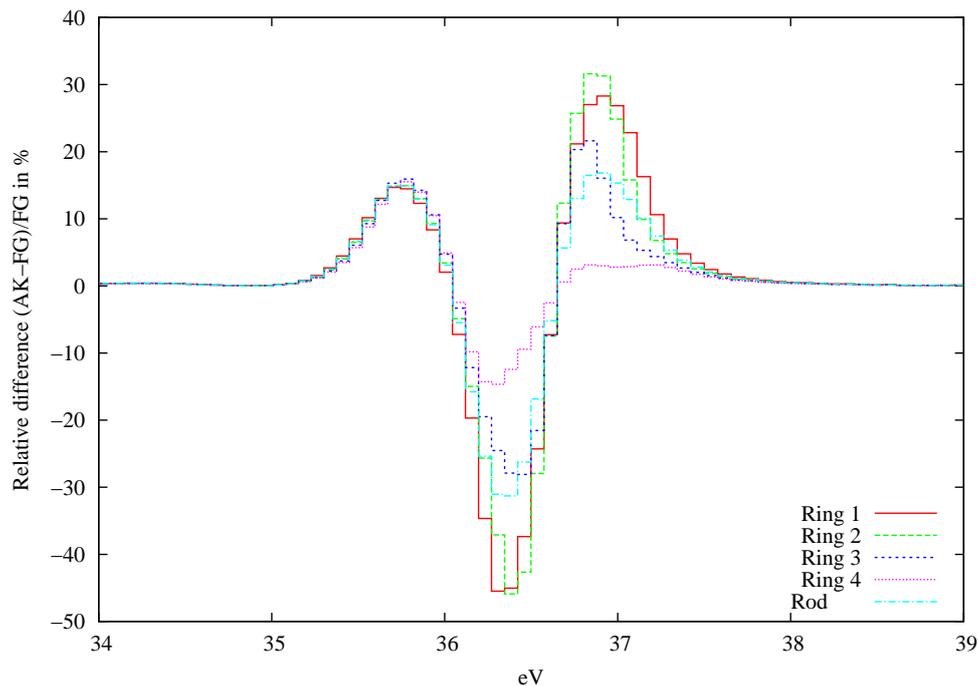

Figure 8. ^{238}U absorption discrepancy between FG model and AK in the resonance around 36.68 eV at 974 K
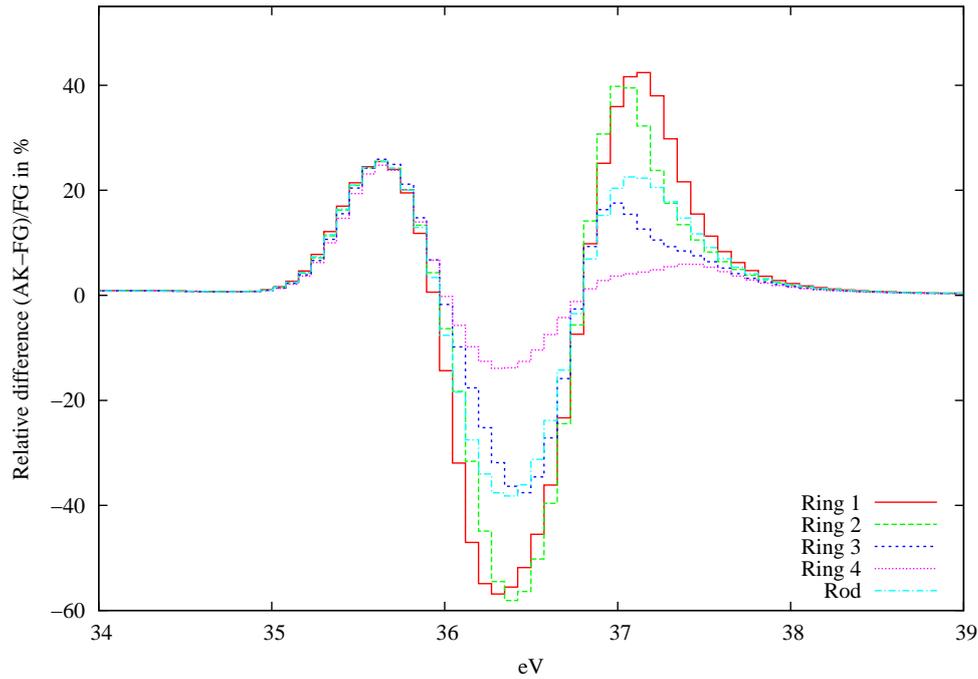
Figure 9. ^{238}U absorption discrepancy between FG model and AK in the resonance around 36.68 eV at 2274 K

5.3. Anisotropic Scattering Analysis

Figure 10 shows the difference on the absorption rates at 974 K in the first and the fourth ring for P_0 and P_5 scattering orders. Scattering anisotropy has almost no effect on the right side of the resonance and a slight effect on the left side. The influence of this parameter on the FG kernel is discussed in Fig. 11 for the four rings and the rod through the following differences $(\frac{AK-FG}{FG})_{P_0} - (\frac{AK-FG}{FG})_{P_5}$, noted in the legend $\Delta(P_0 - P_5)$. The highest difference is equal to -2.5 % and is localized in the left side of the resonance wing where the backscattering effect is amplified by the FG model. However, for the ^{238}U in this energy range the angular distribution is not very peaked and is already well represented by a P_1 development.
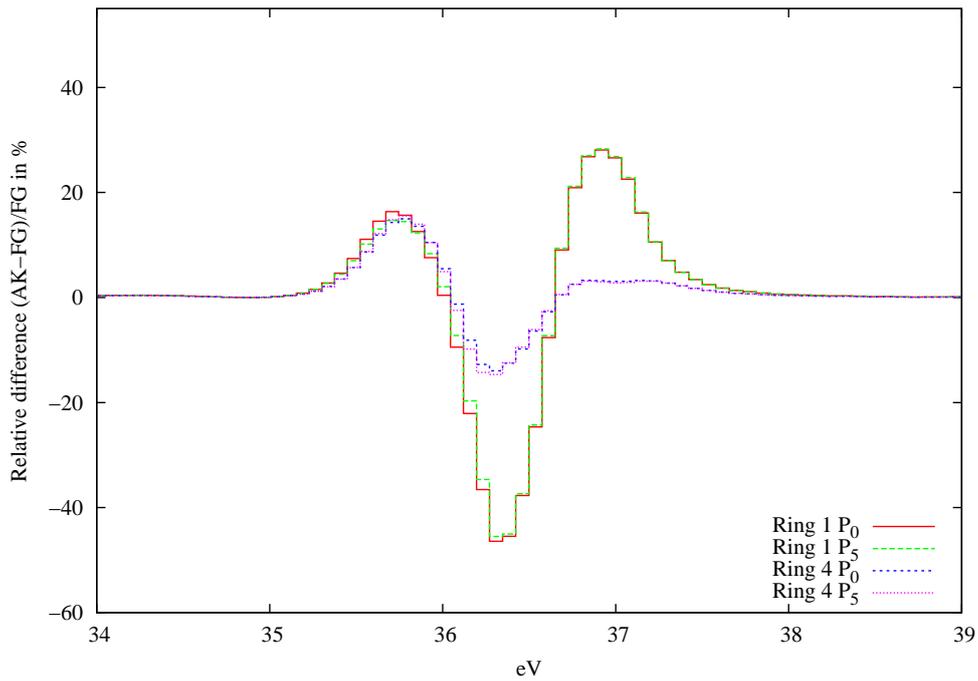
Figure 10. ^{238}U absorption discrepancy at 974 K between FG model and AK for P_0 and P_5 anisotropic scattering order in the resonance at 36.68 eV
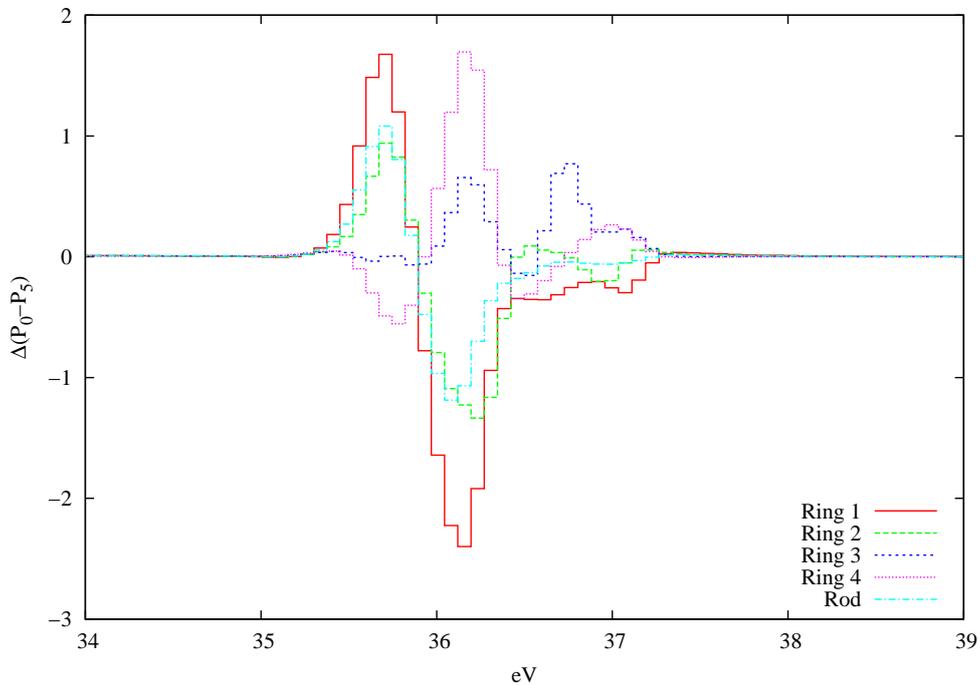

Figure 11. Differences $\Delta(P_0 - P_5) = (\frac{AK - FG}{FG})_{P_0} - (\frac{AK - FG}{FG})_{P_5}$ on the ^{238}U absorption discrepancy at 974 K between FG model and AK in the resonance at 36.68 eV

6. CONCLUSION

Since the beginning of the multigroup transport calculation, the thermal energy range has been continuously extended up too few eV but the use of an inconsistent free gas model above the thermal cut was not questioned until 1990's. It was implicitly admitted that the static model together with the Doppler broadened cross-section gave results precise enough. The new requirements of accuracy in numerical calculations, namely errors lower than 0.1% on keff or 1% on resonant absorption rates, justify the use of more sophisticated models. In this context, this work discusses the effects of the FG kernel developed by Sanchez on reactor physics calculations. Homogeneous medium tests point out the increase of the absorption rates in the left wing of the resonances due to the upscattering produced by the new kernel. Heterogeneous tests show that the absorption in the left wing of the resonances is mostly affected by the scattering anisotropy.

In perspective, the new standard processing of nuclear data for reactor physics analysis should include the consistent FG model for the calculation of the pointwise double-differential scattering kernel $\sigma_s(E, E', \mu_L)$. However, its use will not be so straightforward in the routine production of the APOLLO2 multigroup libraries, except starting with the less time consumming but not rigorous calculation of the pointwise P0 component of the kernel $\sigma_s(E, E')$, because of its high computational cost and a preliminary review of the standard NJOY routines will certainly be required. The optimization of the incident energy grid and the parallelisation of the processes are strategies to be explored in the future.

ACKNOWLEDGMENTS

REFERENCES

[1] E. Fermi. *Collected Papers*, volume Vol. I, Italy 1921-1938. The University of Chicago Press (1962).

[2] E.P. Wigner and J.E. Wilkins Jr. *Effect of the temperature of the moderator on the velocity distribution of neutrons with numerical calculations for H as moderator*. *Technical Report AECD-2275*, United States Atomic Energy Commission (1944).

[3] L. Finkelstein. "Temperature effect on neutron scattering kernels." In: *Neutron thermalization and reactor spectra*, volume 1 (I. A. E. Agency, editor). Ann Arbor (1967).

[4] G. L. Blackshaw and R.L. Murray. "Scattering functions for low-energy neutron collisions in a maxwellian monoatomic gas." *Nucl. Sci. and Eng.*, **27**: pp. 520–532 (1967).

[5] R. Sanchez and M. Ouisloumen. "A model for neutron scattering of heavy isotopes that accounts thermal agitation effects." *Nucl. Sci. and Eng.*, **107**: pp. 189–200 (1991).

[6] Richard Sanchez, Claire Hewko and Simone Santandrea. "Numerical Computation of Doppler-Broadening in the Resonance Domain." In: *International Conference on Mathematics and Computational Methods Applied to Nuclear Science & Engineering*. Sun Valley, Idhao, USA (2013).

[7] R. Dagan. "On the use of $S(\alpha, \beta)$ tables for nuclides with well pronounced resonances." *Annals of Nuclear Energy*, **32**: pp. 367–377 (2005).

[8] Deokjung Lee, Kord Smith and Joel Rhodes. "The impact of U238 resonance elastic scattering approximations on the thermal reactor Doppler reactivity." *Annals of Nuclear Energy*, **36(3)**: pp. 274–280 (2009).

[9] R. MacFarlane and D. Muir. "The njoy nuclear data processing system, version 91." *LA12740-M (October 1994) and RE MacFarlane:" README0"(December 31, 1999)* (1994).

[10] E. Brun, E. Dumonteil, F.X. Hugot, N. Huot, C. Jouanne, Y.K. Lee, F. Malvagi, A.Mazzolo, O. Petit, J.C. Trama and A. Zoia. "Overview of TRIPOLI-4®version 7 Continuous-energy Monte Carlo Transport Code." In: *In International Conference on Advancesin Nuclear Power Plants*. Nice, France (2011).

[11] P. Mosca, C. Mounier, R. Sanchez and G. Arnaud. "An Adaptive Energy Mesh Constructor for Multigroup Library Generation for Transport Codes." *Nuclear Science and Engineering*, **Volume 167(1)**: pp. Pages 40–60 (January 2011).

[12] Andrea Zoia, Emeric Brun, Cédric Jouanne and Fausto Malvagi. "Doppler broadening of neutron elastic scattering kernel in TRIPOLI-4®." *Ann. Nucl. Energy*, **54**: pp. 218–226 (2013).

[13] S. Mengelle. *APOLLO2 : Calcul de référence utilisant un maillage énergétique fin*. Ph.D. thesis, Université Paris XI Orsay (1995).

[14] N. Hfaiedh and A. Santamarina. "Determination of the optimised SHEM mesh for neutron transport calculation." In: *American Nuclear Society Topical Meeting in Mathematics and Computations, Supercomputing, Reactor Physics and Nuclear and Biological Applications*. Avignon, France (2005).

[15] R. Sanchez et al. "APOLLO2 YEAR 2010." *Nuclear Engineering and Technology*, **42**: pp. 474–499 (2010).